Spatial fractionation of the dose in heavy ions therapy: an optimization study.

W. González and Y. Prezado*

IMNC-UMR 8165, CNRS; Paris 7 and Paris 11 Universities,

15 rue Georges Clemenceau, 91406 Orsay Cedex, France

(Dated: March 28, 2018)

Abstract

Purpose: The alliance of charged particle therapy and the spatial fractionation of the dose, as in minibeam or Grid therapy, is an innovative strategy to improve the therapeutic index for the treatment of radioresistant tumors. The aim of this work was to assess the optimum irradiation configuration in heavy ion spatially fractionated radiotherapy (SFRT) in terms of ion species, beam width, center-to-center distances, and linear energy transfer (LET), information that could be used to guide the design of the future biological experiments. The nuclear fragmentation leading to peak and valley regions composed of different secondary particles, creates the need for a more complete dosimetric description that the classical one in SFRT.

Methods: Monte Carlo simulations (GATE 6.2) were performed to evaluate the dose distributions for different ions, beam widths and spacings. We have also assessed the 3D-maps of dose-averaged LET and proposed a new parameter, the peak-to-valley-LET ratio, to offer a more thorough physical evaluation of the technique.

Results: Our results show that beam widths larger than 400 μm are needed in order to keep a ratio between the dose in the entrance and the dose in the target of the same order as in conventional irradiations. A large ctc distance (3500 μm) would favor tissue sparing since it provides higher PVDR, it leads to a reduced contribution of the heavier nuclear fragments and a LET value in the valleys a factor 2 lower than the LET in the ctc leading to homogeneous distributions in the target.

Conclusions: Heavy ions MBRT provide advantageous dose distributions. Thanks to the reduced lateral scattering, the use of submillimetric beams still allows to keep a ratio between the dose in the entrance and the dose in the target of the same order as in conventional irradiations. Large ctc distances (3500 μm) should be preferred since they lead to valley doses composed of lighter

nuclear fragments resulting in a much reduced dose-averaged LET values in normal tissue, favoring its preservation. Among the different ions species evaluated, Ne stands out as the one leading to the best balance between high PVDR and PVLR in normal tissues and high LET values (close to 100 keV/μm) and a favourable oxygen enhancement ratio in the target region.

Keywords: Hadron Minibeam radiation therapy, Grid therapy, Monte Carlo simulations

*Electronic address: prezado@imnc.in2p3.fr

I. INTRODUCTION

The use of the spatial fractionation of the dose in charged particle therapy is a new therapeutic approach [1], [2] and [3] to overcome the main limitation in radiotherapy (RT), namely the normal tissue tolerances. Spatial fractionated radiotherapy (SFRT) started soon after the birth of RT with the aim of reducing skin damage when deep seated tumors were to be treated with the existing orthovoltage machines. This approach, called GRID therapy [4], is currently used clinically at few hospitals using megavoltage (MV) photon beams delivered by medical Linacs [5], [6] and [7]. GRID therapy (GRT) has been successfully used to deposit high doses in the treatment of bulky tumors, for which conventional approaches fail in their management [6], [7] and [8]. However, the important lateral scattering of MV beams and the relative low fluence of Linacs limits the gain of this technique [9]. The extremely high fluence of non-divergent kilovoltage beams provided by third generation synchrotron sources triggered the alliance of the spatial fractionation of the dose with the use of very narrow (submillimetric) beams, as in microbeam and minibeam radiation therapies [10], [11] and [12]. The use of small field sizes allows to better exploit the dose-volume effects [13], further increasing the normal tissue sparing. Indeed, extremely high normal tissues dose tolerances have been observed in animal studies [10], [14], [15], [11] and [16]. Tumor growth delay in aggressive animal tumor models was also observed [17], [18], [19], [20] and [21]. These outcomes seem to be the result of the participation of some biological mechanisms (not well understood yet) different from those ones in 'standard' RT.

A further improvement of therapeutic index could be achieved by joining the advantages of the spatial fractionation of the dose to the high dose conformity and increased relative biological effectiveness (RBE) of heavy ions. The exploration of this new approach has re-

cently started. Different particles have been studied. Proton MBRT [2] has already been implemented at a clinical center [22] and the first biological experiments confirms a remarkable gain in normal tissue tolerances [23] and [24] reported the evaluation (Monte Carlo simulations) of the broadening in water of several light ions (from protons to ^{7}Li). Among the different types of ion species, carbon ions are considered to have optimal properties in terms of superior physical and biological characteristics [25]. The results of the recent studies on carbon MBRT from dosimetric [26], [27] and biological point of view [1], encourages a further exploration of this approach. Due to their increased linear energy transfer, heavier ions, like oxygen, are considered specially promising for the treatment of hypoxic tumors, which remains one of the major challenges in radiotherapy (RT). Radiobiological findings in the laboratory indicated that resistant cells of hypoxic tumors could be effectively destroyed with very heavy ion beams, such as silicon and argon [28]. However, clinical results with a few patients performed with argon in 1979 and with silicon in 1982 lead to adverse late tissue results, and the use of these beams was discontinued. Nevertheless, the gain in tissue sparing that might be provided by the use minibeam radiation therapy might allow profiting from the remarkable effectiveness of very heavy ions. This could offer a new hope for aggressive hypoxic tumors, whose treatment with conventional methods is very limited. The advantageous dose distributions obtained in the very first Monte Carlo (MC) study [3] support the further exploration of this avenue.

This work is devoted to the assessment of optimum irradiation configurations in heavy ion spatially fractionated RT (SFRT) in terms of ion species, beam width and shape, and center-to-center (ctc) distance, that could be used to guide the design of future biological experiments. In order to maximize the dose volume effects, we have evaluated for each ion the minimum beam width that could be used without significantly degrading the ratio

between the entrance dose and the dose at the Bragg peak [29].

In SFRT, the resulting dose profiles follow a pattern of peaks and valleys, with high doses along the primary beam path (peaks) and low doses in the space between them (valleys). Previous experiments at synchrotrons (x-rays) indicate that normal tissue sparing seems to benefit from a high peak-to-valley dose ratio (PVDR) and low valleys while low PVDR and high doses to the tumor favor tumor control [18]. PVDR is used as an important dosimetric variable in x rays SFRT. However, due to nuclear fragmentation, PVDR or valley dose, may not provide a thorough description in heavy ion SFRT. Indeed, the produced nuclear fragments are going to fill the valleys, which will then be composed of a mix of particles. The same PVDR or even the same valley dose can correspond to different composition of fragments leading to different effects on normal tissues. This is usually taken in consideration in heavy ion therapy by using RBEs. However, uncertainty on the RBE is often quoted as a major hindrance to a widespread use of heavy ions in radiotherapy and is a source of concern for the potential late effects. For instance, C-ions have been used very little in pediatric patients mostly for the concern about high risk of secondary cancers. In addition, the expected radiobiological features of SFRT are so different from those of 'standard' irradiations, probably including some non-targeted effects that the radiobiological effect cannot be assessed by means of established RBEs of 'standard' hadron therapy (seamless beam irradiation). Biological experiments are needed to assess the effectiveness of this approach and reconstruct the complete picture. In the meantime, maps of dose-averaged Linear Energy Transfer (LET) can be reliably quantified by means of MC simulations [30] and used to predict the regions of expected higher biological effect. LET describes the density of ionization and, therefore, the probability of the damage. New parameters based on dose-averaged LET, more suitable for a quantitative physical description of heavy ion therapy SFRT, have

been defined and evaluated.

Since our approach is especially suitable for tumors for which pulmonary and/or cardiac cycles (target motions) have minimal effects, in particular, for presently difficult-to-treat neurological indications, our study was focused on parameters adequate for brain tumor treatments.

II. MATERIALS AND METHODS

A. Monte Carlo simulations

The code GATE (version 6.2) [31] was employed in this work. GATE is an open source MC simulation platform based on GEANT4 (version 4.9) [32] enabling the modeling of emission and transmission tomography, and radiotherapy. The option 3 of the electromagnetic standard physics package for GEANT4 and the recommended hadronic physics list for carbon were used [32]. A range cut value of 50 μm was used for all particles in the water phantom. The number of primary particles employed was 4×10^9 ions. This leads to 1% of maximum uncertainty (with a cover factor $k = 2$).

A magnetic collimation was assumed to generate minibeams of six different ions (^{12}C, ^{16}O, ^{20}Ne, ^{28}Si, ^{40}Ar and ^{56}Fe). Two different irradiation geometries were considered: rectangular (1D-Grid or minibeams (MBRT)) and squared (2D-Grid (GRT)) beams, with dimensions ranging from 100 μm $\times$ 2 cm to 700 μm $\times$ 2 cm in the first case and from 300 μm $\times$ 300 μm to 1000 μm $\times$ 1000 μm, in the second case. See figure 1. The sources were located at the phantom entrance. The beams impinged on a cylindrical water phantom whose size (height and diameter of 16 cm) mimics the human head and it has been used in previous dosimetric studies [3] and [27]. A virtual tumor (2 cm $\times$ 2 cm $\times$ 2 cm) was placed at 7

cm-depth. A realistic angular spread of 3 mrad [33] and [34] and Gaussian shape were considered. The dose accumulation voxels had dimensions of 60 μm $\times$ 2 mm $\times$ 1mm and 60 μm $\times$ 60 μm $\times$ 1mm for MBRT and GRT, respectively. To save computation time only one single beam was simulated and the dose distributions were evaluated as the sum of the contributions of each individual minibeam to cover the virtual tumor (2 cm $\times$ 2 cm).

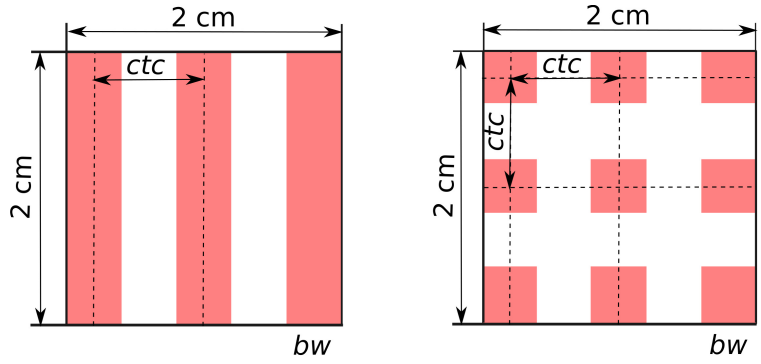

FIG. 1: Scheme representing the geometrical parameters in MBRT (left) and in GRT (right). *ctc* refers to the distance between two consecutive beam centers and *bw* to the beam width.

First, pristine Bragg peak curves were calculated to determine the minimum beam width (*bw*) for each ion/configuration by evaluating the ratio between the dose at the entrance and the dose at the Bragg Peak. A maximum ratio of around 25 %, similar to the ones that would be obtained in conventional (broad beam) irradiations [35], was used as a criterion. Then, SOBP irradiations covering the target homogeneously in depth were also simulated. With that aim 50 monoenergetic ion beams were weighted using the method described by Jette and Chen [36]. The table II A show the minimum and maximum energies used for each ion.

The peak-to-valley dose ratio as a function of depth was assessed for each ion and its corresponding minimum width. As explained in the Introduction, we have also evaluated the dose-averagde LET as a dosimetry parameter that may provide a more complete physical

TABLE I: Minimum and maximum energies used to generate SOBP for each ion.

	^{12}C	^{16}O	^{20}Ne	^{28}Si	^{40}Ar	^{56}Fe
Emin (MeVu^{-1})	164.6	195.5	221.2	270.4	297.5	382.8
Emax (MeVu^{-1})	194.2	230.6	276.0	319.0	351.0	450.0

description of heavy ion SFRT. LET describes the energy transferred into a narrow region around the primary ion track. While the LET of a pure beam of ions with a fixed energy is well defined, the LET of a mixed radiation field is more complex. The reason for that is, that in a mixed radiation field, LET has to be averaged over the different ions contributing. This is often done by using the so-called dose-averaged LET, where the LET of each particle is weighted according to the dose it is contributing. GATE v8.0 was used to calculate 3D maps of unrestricted dose-averaged LET. In particular, we have evaluated the dose-averaged LET in the peak and valley regions as a function of depth. We have also introduced a new parameter, called Peak-to-valley-LET-ratio (PVLR), to give a more thorough dosimetric quantification of this approach. Two different (*ctc*) distances have been considered: a *ctc* leading to LET-homogeneous profiles in the target and a *ctc* that has been shown to minimize the contribution of heavy nuclear fragments to the valleys, i.e. 3500 μm [3] and [27].

III. RESULTS AND DISCUSSION

In this section, the results of the assessment of the minimum *bw* for each ion and configuration are reported first. Then, PVDR values as a function of depth corresponding to that *bw* will be shown. Finally, dose-averaged LET distributions will be presented.

In order to assess the minimum *bw* for each ion for the two irradiation geometries under

TABLE II: Optimum beam width determined for each ion.

	^{12}C	^{16}O	^{20}Ne	^{28}Si	^{40}Ar	^{56}Fe
MBRT *bw* (μm)	600	600	500	500	400	400
GRT *bw* (μm)	900	900	800	800	700	700

consideration, MBRT and GRT, depth doses curves were evaluated following the dosimetry criterium explained in section II. See figure2. The shape of the depth dose curves significantly change when very small *bw* are used: a (very) high ratio of lateral scattered dose with respect to the dose deposited in the primary trajectory of the beam, resulting in the loss of the characteristic Bragg peak shape and its advantages. The same reason explains the difference between MBRT and GRT configurations. Whether high entrance-to-Bragg peak dose ratio and the relative higher presence of nuclear fragments in the valleys could be compensated in terms of tissue sparing by distinct biological mechanisms being activated when very narrow beams ($\leq$ 100 μm) are used is yet to be established by biological experiments. Table III shows the results on the optimum (minimum) *bw* for each beam and configuration.

As expected the *bw* is smaller for the heaviest ions due to the reduced lateral scattering. By using those minimum *bw* we have then assessed the PVDR, as well as LET maps. SOBP have been used for that evaluation. Figure 3 shows examples of SOBP for Si ions for MBRT and GRT configurations. The normal tissue at the entrance receive between 70-75 % in MBRT and 65-70 % in GRT of the average dose in the SOBP for the different ions. Similar values (70 %) have been reported in 'standard' ion therapy [37].

As explained in Materials and Methods, two different *ctc* were considered: a *ctc* that has been shown to minimise the contribution of heavy nuclear fragments to the valleys, i.e., 3500

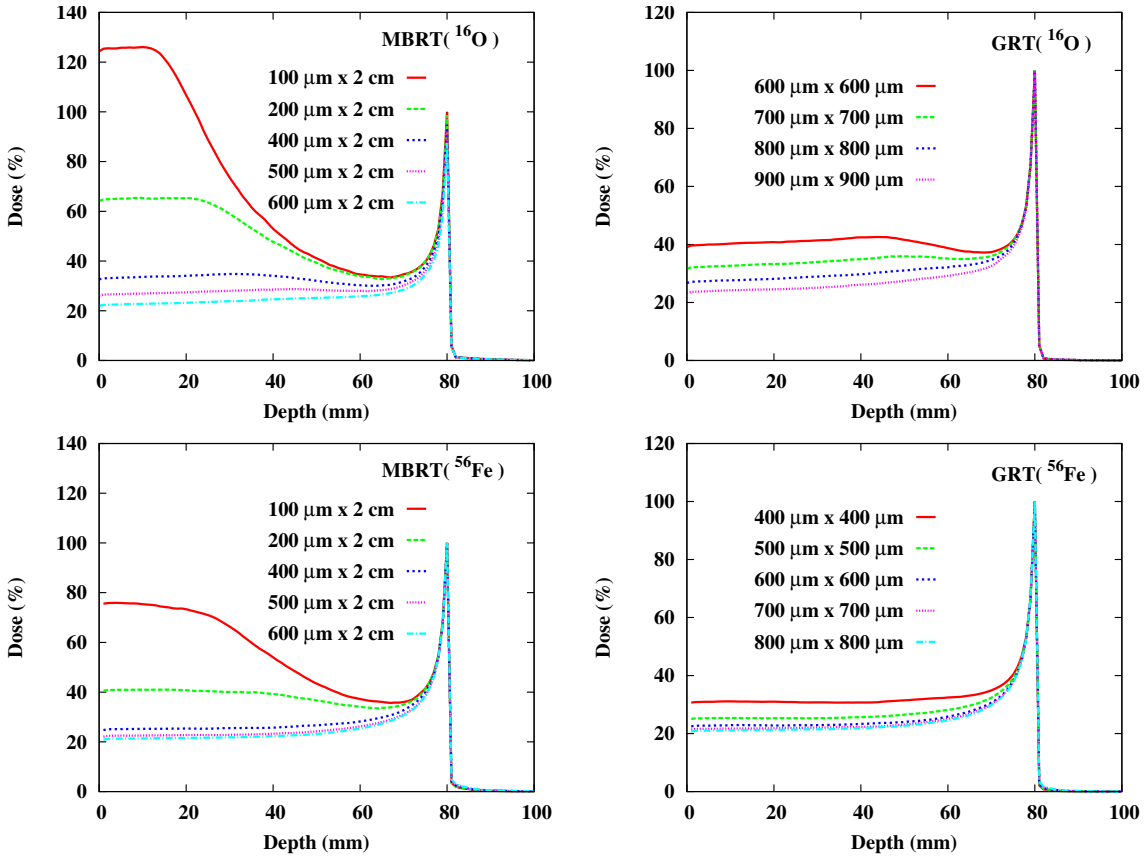

FIG. 2: Depth dose curves resulting from the irradiation (Pristine peaks) with beams of different widths. The upper row corresponds to curves of oxygen ions, the lower one to iron. The left and right columns depict the curves for MBRT and GRT irradiations, respectively. The values were normalized to the maximum value.

μm [3] and [27] and a *ctc* leading to LET-homogenous profiles in the target. Concerning the latter, an empirical relation between the *ctc* and the *bw* was found:

$$ctc = 2 \times bw, \quad \text{for MBRT} \tag{1}$$

$$ctc = 2 \times bw - 400\ \mu m, \quad \text{for GRT} \tag{2}$$

Figure 4 shows the PVDR for the different ions, configurations and *ctc* distances. Extremely high PVDR values for a *ctc* of 3500 μm are obtained, similar or equal to previously

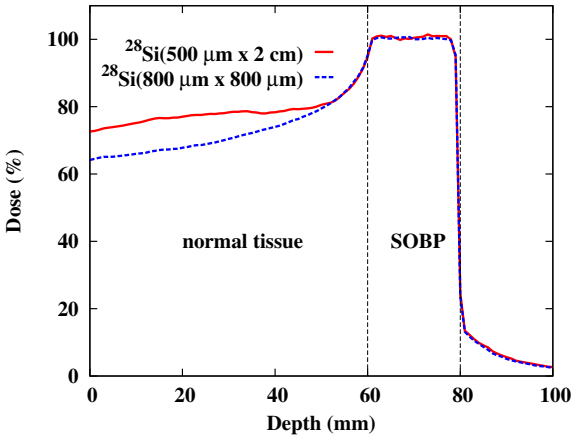

FIG. 3: Percentage depth dose curves for the central peak silicon MBRT (solid line) and GRT (dotted line). The values were normalized with respect to the average dose in the SOBP.

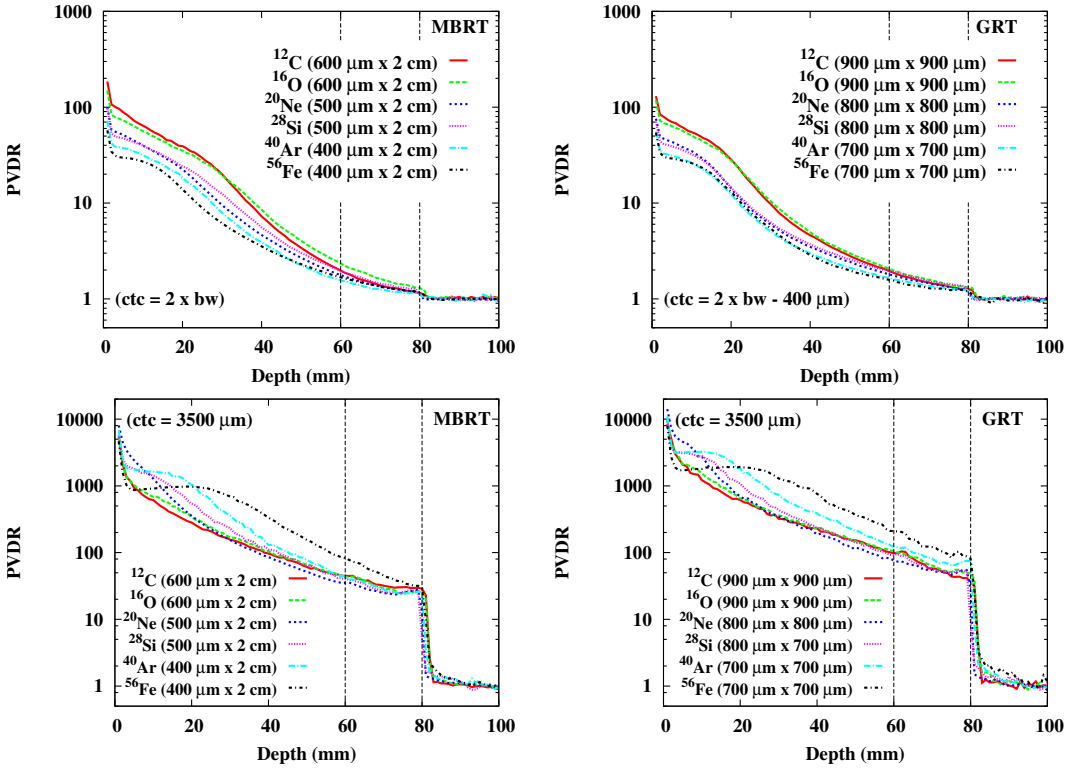

FIG. 4: PVDR as a function of depth for each ion. The left and right columns corresponds to MBRT and GRT, respectively. The upper row shows the results when the *ctc* leading to in the LET-homogenous profiles in the target is used, the lower row depicts the values for a *ctc* of 3500 μm.

156 published works [3] and [27]. For the narrowest *ctc* distances, PVDR values in the first 2

cm are similar to those obtained in x-rays and proton MBRT [22], [38]. Values comparable to GRID therapy are achieved for depths from 2 to 5 cm [39]. A quasi homogeneous dose distribution is obtained in the target (from 6 to 8 cm depth) with only one array, without interlacing.

The narrower *ctc* leads to similar values for each ion in MBRT and GRT configurations. The lowest PVDR are obtained for the heaviest ions. The opposite situation is found when a *ctc* of 3500 μm is used. Larger PVDR are obtained in GRT than in MBRT when a *ctc* of 3500 μm is used.

Figure 5 shows the ratio between the peak and valley dose-averaged LET (PVLR). The highest values are obtained in the first millimeters, being Fe the ion providing the highest PVLR (205 ± 2 in MBRT and 200 ± 2 in GRT). In normal tissues in the beam path, the heaviest the ion, the highest the PVLR. The ratio between the PVLR in the entrance and the target region being as well the highest for the heaviest ion. A factor 100 is obtained in the entrance between the PVLR for Fe and C. PVLR as a function of depth for lightest ions, like carbon and oxygen have a soft trend, being in the entrance approximately double the value in the target. The curves of PVLR as a function of depth are very similar in the two configurations, MBRT and GRT, being slightly higher for GRT. As opposed to PVDR, PVLR does not significantly change with *ctc*. PVLR in the target is not homogeneous to the 3500 μm *ctc* setup. The trend of the curves can be explaining using the dose-averaged LET in the valleys (figure 7), to this setup, the trend of the curves are different that the trend of the curves to the small *ctc* setup.

Figures 6 and 7 show the dose-averaged LET in the peaks and the valleys, respectively. Concerning the LET in the peaks, there are not significant differences between MBRT and GRT, not variation with the *ctc*. In contrast, LET increases with the atomic number of the

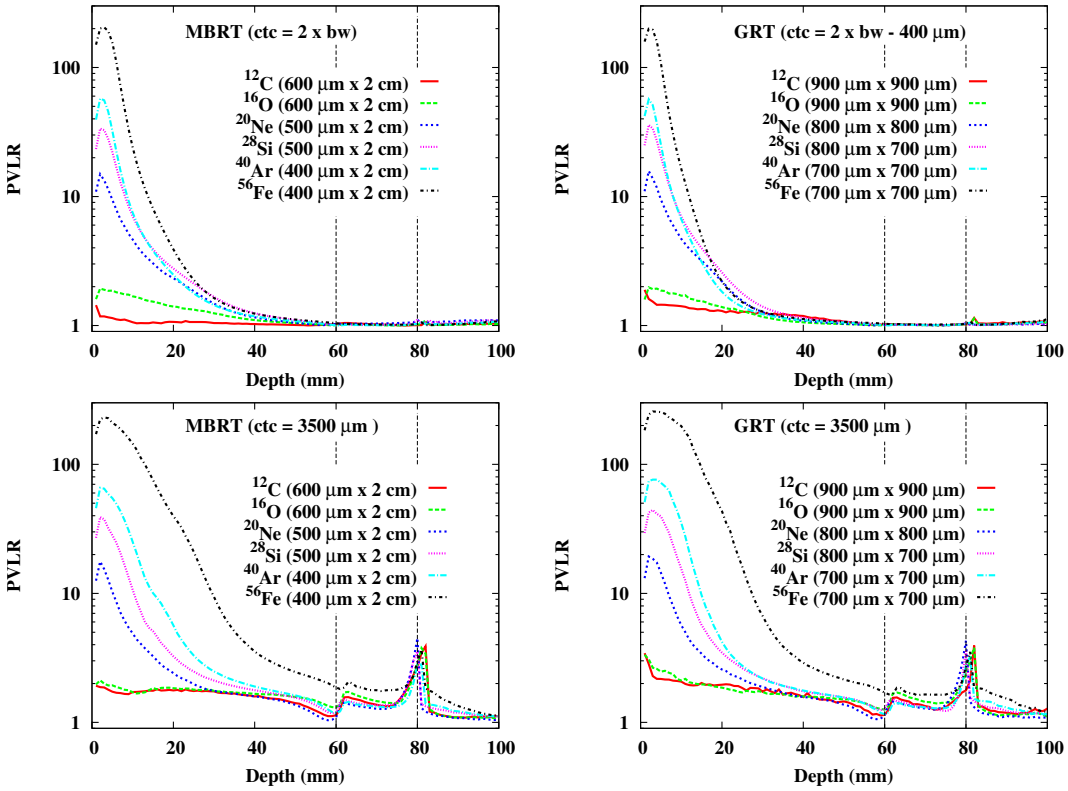

FIG. 5: PVLR as a function of depth for each ion. The left and right columns corresponds to MBRT and GRT, respectively. The upper row shows the results when the ctc leading to in the LET-homogenous profiles in the target is used, the lower row depicts the values for a *ctc* of 3500 μm.

ion, as expected.

In 'standard' hadron therapy (non spatially fractionated), LET values of about 200 keV/μm produce the largest biological effectiveness [40]. An "overkill" effect is reported for LET higher than 200 keV/μm for ^{12}C ions. Some works [41] indicate that the exclusion of non-hit fraction in the calculation of surviving fraction partially prevented the fall of biological effectiveness when LET exceeded 200 keV/μm. The presence of non-hit cells among hit cells is one of the features characteristic for exposure to very high-LET heavy ions. Mehnati *et al.* also suggest that bystander effect may occur in non-hit cell. The expected radiobiological features of minibeam radiation therapy are so different from those

of 'standard' RT, including non-targeted effects (see Y. Prezado *et al.* 2015), that the radiobiological effect cannot be assessed by means of established RBEs of 'standard' hadron therapy (broad beam irradiation). It could be that the fact of having more severe damage in fewer sites triggers a more important contribution of non-targeted effects. Whether in these conditions a possible overkill effect in the distal part of the Bragg peak would be totally maintained or compensated by other phenomena appearing in spatially fractionated techniques, it is yet to be explored.

Values lower than 200 keV/μm are found for all ions except Fe and the distal part of the SOBP of Si and Ar. Whether an overkill effect of the same magnitude than in 'standard RT' would start participating in this technique is yet to be assessed.

Valleys are believed to be (main) responsible for tissue sparing [18]. Low LET values in the valleys could then favor normal tissue preservation. The shape of the LET curves is similar for MBRT and GRT. A smooth variation of the dose-averaged LET as a function of depth is obtained for carbon and oxygen ions. The values for carbon are lower than those encountered in clinics. In contrast, a continuous increase is observed for the heavier ions, with a very high gradient in the first centimeters. An interesting feature is the fact that the LET values for Ne and heavier ions are lower than those of carbon ions in the first centimeter, which would favor normal tissue preservation. The depth where the trend is reversed depends on *ctc* (the larger the *ctc*, the deeper the point) and on ion (the heavier the ion, the deeper the point). The reason is the heavier the primary ion is, the higher the proportion of heavier fragments (high LET), whose angular distribution, mainly determined by reaction kinematics, will then be more forward directed than lighter products. Consequently, their dose deposition will occur deeper. In normal tissues, all ions but Fe, lead to LET values lower than 100 KeV/μm. Superior values are considered to lead to an RBE higher than one

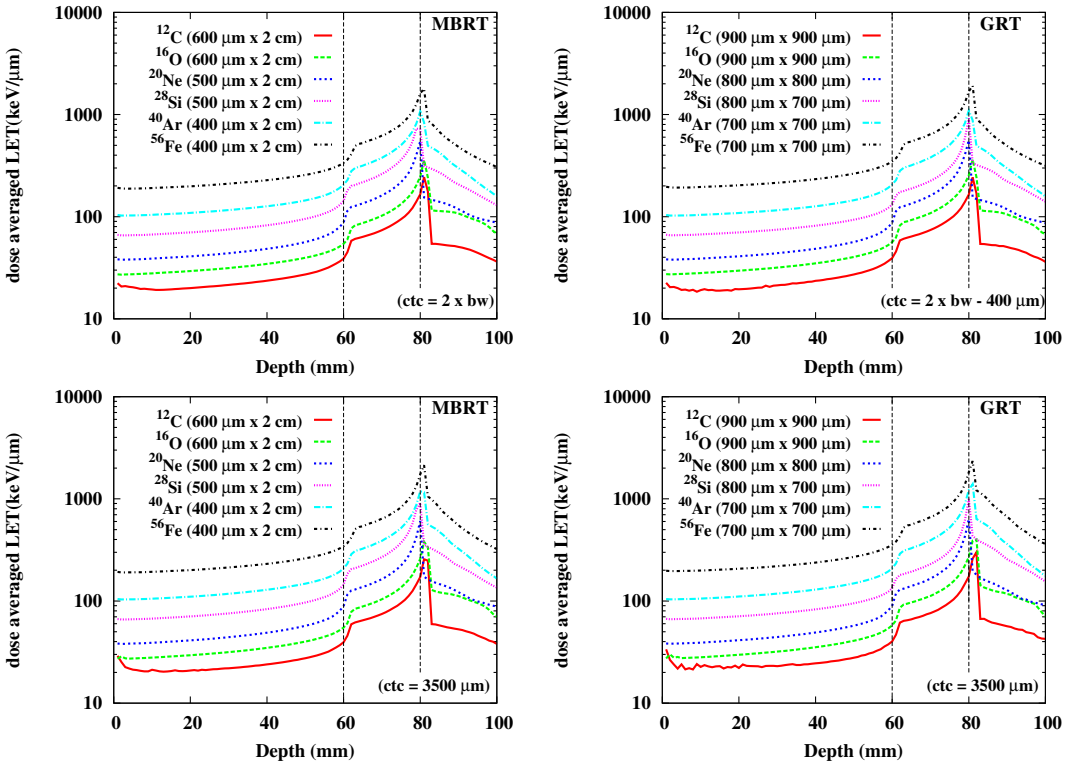

FIG. 6: Dose-averaged LET (peak region) as a function of depth for the different ions. The left and right column corresponds to MBRT and GRT irradiations, respectively. The upper row shows the results when the ctc leading to in the LET-homogenous profiles in the target is used, the lower row depicts the values for a *ctc* of 3500 μm.

[42]. In the target area, Ne and lightest ions provide LET values lower than 200 keV/μm at all depths. LET values are a factor 2 smaller when the 3500 μm *ctc* is used. Not significant differences are observed between MBRT and GRT configurations.

Among the different ions, Ne could offer a good compromise since they lead to high PVDR and PVLR in normal tissues, LET values in the valleys lower than carbon in the first centimeter, remaining below 30 keV/μm in normal tissues (up 6 cm depth) and providing values close to 100 keV/μm in the target region. In addition, Ne provides a lower oxygen enhancement ratio (OER) than lighter ions, which is advantageous for the treatment of

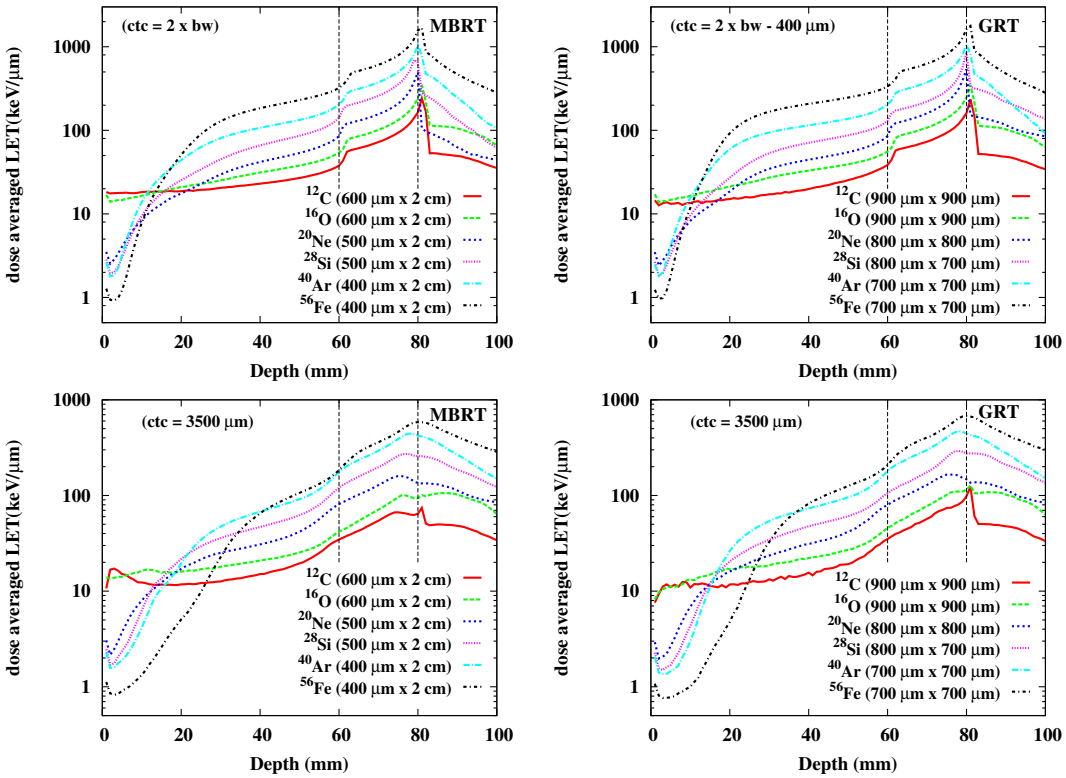

FIG. 7: Dose-averaged LET (valley region) as a function of depth for the different ions. The left and right column corresponds to MBRT and GRT irradiations, respectively. The upper row shows the results when the ctc leading to in the LET-homogenous profiles in the target is used, the lower row depicts the values for a *ctc* of 3500 μm.

hypoxic tumors.

The larger *ctc* leads to higher PVDR and reduced valley doses, with a lower contribution of heavier nuclear fragments to the valleys [3], [27] leading to a factor 2 decrease in the dose averaged LET in normal tissues. The PVLR in the target is lower than 2 (except for Fe), so quasi homogeneous.

Concerning the differences between GRT and MBRT, the main difference is that GRT leads to higher PVDR than MBRT a factor 1.6, however the minimum beam width 1.5 times larger, which might reduce the tissue tolerances.

Although only biological experiments can establish the most favorable configuration, the results obtained in the physical study suggest that Ne MBRT with beam width of 500 μm $\times$ 2 cm and a *ctc* of 3500 μm could be the best candidate. Figure 8 shows a 2D dose map for this case.

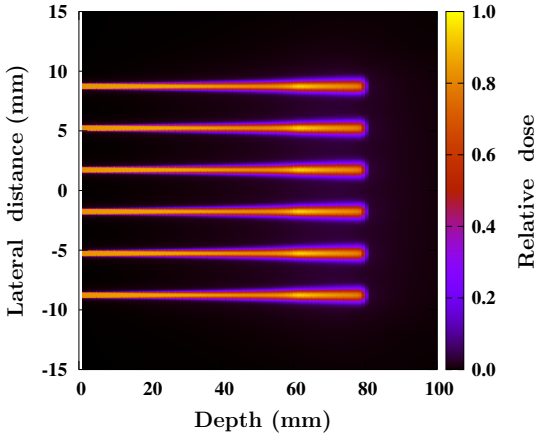

FIG. 8: 2D dose map for the MBRT with beam width of 500 μm $\times$ 2 cm and a *ctc* of 3500 μm .

IV. CONCLUSIONS

Heavy ions minibeam or Grid therapy is a new approach for the treatment of radioresistant tumors. The normal tissue preservation that could be offer by this strategy would allow a dose escalation in the tumor, and therefore, a higher tumor control may be expected. This work aimed at the optimization of the irradiation configuration in terms of ion species, beam width, beam spacing and LET-maps. The use of submillimetric beams still allows to keep a ratio between the dose in the entrance and the dose in the target of the same order as in conventional irradiations. MBRT permits the employment of thinner beams than GRT. Large ctc distances (3500 μm) should be preferred since they lead to valley doses composed of lighter nuclear fragments resulting in a much reduced dose-averaged LET values in normal tissue, favoring its preservation. However, preclinical studies evaluating tumor response will

be the ones providing the ultimate determination of the most effective ctc distance for tumor control. Among the different ions species evaluated, Ne stands out as the one leading to the best balance between high PVDR and PVLR in normal tissues and high LET values (close to 100 keV/μm) and a favorable OER in the target region. Although biological experiments are warranted to confirm these conclusions, the results of this work may be used to guide the future biological studies.

Acknowledgment

The authors acknowledge the calculation time granted at Centre de Calcul de Lyon (IN2P3) and at Grand Equipement National de Calcul Intensif (in particular at the supercomputer Curie of CEA). We warmly thank the access to Castilla y León Supercomputing Center (Calendula) awarded by the Red Española de Supercomputación. We also acknowledge PRACE for awarding us access to resource MareNostrum Barcelona Supercomputing Center based in Spain.

[1] F. A. Dilmanian, A. Rusek, G. R. Fois, J. Olschowka, N. R. Desnoyers, J. Y. Park *et al.*, "Interleaved Carbon Minibeams: An Experimental Radiosurgery Method With Clinical Potential", Int. J. Rad. Oncol. Biol. Phys. **84**, 514-519 (2012).

[2] Y. Prezado and G. R. Fois, "Proton minibeam radiation therapy: a proof of concept", Med. Phys. **40**, 031712 (2013).

[3] C. Peucelle, I. Martínez-Rovira and Y. Prezado, "Spatial fractionation of the dose using Neon and heavier ions: a Monte Carlo study", Med. Phys. **42**, 5928-5936 (2015).

[4] H. Kohler, "Zur roentiefentherapie mit massendosen", MMW-Fortschr. Med. **56**, 2314-2316 (1909).

[5] M. Mohiuddin, D. L. Curtis, W. T. Grizos and L. Komarnicky, "Palliative treatment of advanced cancer using multiple nonconfluent pencil beam irradiation. A pilot study", Cancer. **66**, 114-118 (1990).

[6] M. Mohiuddin, M. Fujita, W. F. Regine, A. S. Megooni, G. S. Ibbott and M. M. Ahmed, "High-dose spatially-fractionated radiation (grid): a new paradigm in the management of advanced cancers", Int. J. Rad. Oncol. Biol. Phys. **45**, 721-727 (1999).

[7] J. A. Peñagarícano, E. G. Moros, V. Ratanatharathorn, Y. Yan and P. Corry, "Evaluation of spatially fractionated radiotherapy (GRID) and definitive chemoradiotherapy with curative intent for locally advanced squamous cell carcinoma of the head and neck: initial response rates and toxicity", Int. J. Rad. Oncol. Biol. Phys. **76**, 1369-1375 (2010).

[8] J. L. Huhn, W. F. Regine, J. P. Valentino, A. S. Meigooni, M. Kudrimoti and M. Mohiuddin, "Spatially fractionated grid radiation treatment of advanced neck disease associated with head and neck cancer", Technol Cancer Res Treat. **5**, 607-612 (2006).

[9] I. Martínez-Rovira, J. Puxeu and Y. Prezado, "Dose evaluation of Grid Therapy using a 6 MV flattening filter free (FFF) photon beam: a Monte Carlo study", Med. Phys. **44**, 5378-5383 (2017b).

[10] D. N. Slatkin, P. Spanne, F. A. Dilmanian, J. O. Gebbers and J. A. Laissue, "Subacute neuropathological effects of microplanar beams of x-rays from a synchrotron wiggler", Proc. Natl. Acad. Sci. U.S.A. **92**, 8783-8787 (1995).

[11] F. A. Dilmanian, Z. Zhong, T. Bacarian, H. Benveniste, P. Romanelli, R. Wang, J. Welwart, T. Yuasa, E. M. Rosen and D. J. Anschel, "Interlaced x-ray microplanar beams: A radiosurgery

approach with clinical potential" Proc. Natl. Acad. Sci. U. S. A. **103**, 9709-9714 (2006).

[12] Y. Prezado, M. Renier and A. Bravin, "A new method of creating minibeam patterns for synchrotron radiation therapy: a feasibility study", J. Synchr. Radiat. **16**, 582-586 (2009).

[13] J. W. Hopewell and K. R. Trott K R, "Volume effects in radiobiology as applied to radiotherapy", Radiother. Oncol. **56**, 283-288 (2000).

[14] J. A. Laissue, H. Blattmann, M. Di Michiel, D. N. Slatkin, N. Lyubimova, R. Guzman, W. Zimmermann, S. Birrer, T. Bley, P. Kircher, R. Stettler, R. Fatzer, A. Jaggy, H. M. Smilowitz, E. Brauer, A. Bravin, G. LeDuc, C. Nemoz, M. Renier, W. C. Thomlinson, J. Stepanek and H. P. Wagner, "Weanling piglet cerebellum: A surroGATE for tolerance to MRT (microbeam radiation therapy) in pediatric neuro-oncology", Proceeding of SPIE **4508**, 65-73 (2001).

[15] J. A. Laissue, S. Bartzsch, H. Blattmann, E. Bräuer-Krisch, A. Bravin, A. Dalléry, V. Djonov, A. L. Hanson, J. W. Hopewell, B. Kaser-Hotz, J. Keyriläinen, P. P Laissue, M. Miura, R. Serduc, A. E. Siegbahn and D. N. Slatkin, "Response of the rat spinal cord to X-ray microbeams", Radiother. Oncol. **106**, 106-111 (2013).

[16] Y. Prezado, P. Deman, P. Varlet, G. Jouvion, S. Gil, H. C. LeClec', H. Bernard, G. Le Duc and S. Sarun, "Tolerance dose escalation in minibeam radiation therapy applied to normal rat brain: long-term clinical, radiogical and histopathological analysis", Rad. Research. **184**, 314-321 (2015).

[17] J. A. Laissue *et al.*, "Neuropathology of ablation of rat gliosarcomas and contiguous brain tissues using a microplanar beam of synchrotron-wiggler-generated X rays", Int. J. Cancer **78**, 654-660 (1998).

[18] F. A. Dilmanian, T. M. Button, G. Le Duc, N. Zhong, L. A. Peña, J. A. Smith *et al.*, "Response of rat intracranial 9L gliosarcoma to microbeam radiation therapy", Neuro Oncol. **4**, 26-38

(2002).

[19] M. Miura, H. Blattmann, E. Bräuer-Krisch, A. Bravin, A. L. Hanson, M. M. Nawrocky, P. L. Micca, D, N. Slatkin and J. A. Laissue, "Radiosurgical palliation of aggressive murine SCCVII squamous cell carcinomas using synchrotron-generated x-ray microbeams", Br. J. Radiol. **79**, 71-75 (2006).

[20] A. Bouchet, B. Lemasson, G. Le Duc, C. Maisin, E. Bräuer-Krisch, E. A. Siegbahn, L. Renaud, E. Khalil, C. Rémy, C. Poillot, A. Bravin, J. A. Laissue, E. L. Barbier and R. Serduc, "Preferential effect of synchrotron microbeam radiation therapy on intracerebral 9L gliosarcoma vascular networks", Int. J. Rad. Oncol. Biol. Phys. **78**, 1503-1512 (2010).

[21] Y. Prezado, S. Sarun, S. Gil, P. Deman, A. Bouchet and F. Le Duc, "Increase of lifespan for glioma-bearing rats by using minibeam radiation therapy", J. Synchrotron Radiat. **19**, 60-65 (2012).

[22] C. Peucelle, C. Nauraye, A. Patriarca, E. Hierso, E. Fournier-Bidoz, I. Martínez-Rovira and Y. Prezado, "Proton minibeam radiation therapy: Experimental dosimetry evaluation", Med. Phys. **42**, 7108-7113 (2015b).

[23] Y. Prezado, G. Jouvion, A. Patriarca, C. Nauraye, J. Bergs, W. González, C. Guardiola, M. Juchaux, D. Labiod, L. Jourdain, C. Sebrie and F. Pouzoulet, "Proton minibeam radiation therapy spares normal rat brain: Long-Term Clinical, Radiological and Histopathological Analysis", Sci. Rep. **7**, 14403 (2017).

[24] F. A. Dilmanian, J. G. Eley and S. Krishnan, "Minibeam Therapy with protons and Light Ions: Physical Feasibility and Potential to Reduce Radiation Side Effects and to Facilitate Hypofractionation", Int. J. Radiat. Oncol. Biol. Phys. **92**, 469-474 (2015).

[25] T. Okada, T. Kamada, H. Tsuji, J. E. Mizoe, M. Baba, S. Kato, S. Yamada, S. Sugahara,

S. Yasuda, N. Yamamoto, R. Imai, A. Hasegawa, H. Imada, H. Kiyohara, K. Jingu, M. Shinoto and H. Tsujii, "Carbon ion radiotherapy: clinical experiences at National Institute of Radiological Science (NIRS)", J Radiat Res. **51**, 355-364 (2010).

[26] I. Martínez-Rovira, W. González, S. Brons and Y. Prezado, "Carbon and oxygen minibeam radiation therapy: experimental dosimetric evaluation", Med. Phys. **44**, 4223-4229 (2017a).

[27] W. González, C. Peucelle and Y. Prezado, "Theorical dosimetric evaluation of carbon and oxygen minibeam radiation therapy", Med. Phys. **44**, 1921-1929 (2017).

[28] J. R. Castro, D. E. Linstadt, J. P. Bahary, P. L. Petti, I. Daftari, J. M. Collier, P. H. Gutin, G. Gauger and T. L. Philips, "Experience in charged particle irradiation of tumors of the skull base: 1977 - 1992", Int. J. Rad. Oncol. Biol. Phys. **29**, 647-655 (1994).

[29] I. Martínez-Rovira, G. Fois and Y. Prezado, "Dosimetric evaluation of new approaches in GRID therapy using nonconventional radiation sources", Med. Phys. **42**, 685-693 (2015).

[30] I. Kantemiris, P. Karaiskos, P. Papagiannis and A. Angelopoulos, "Dose and dose averaged LET comparison of ^{1}H, ^{4}He, ^{6}Li, ^{8}Be, ^{10}B, ^{12}C, ^{14}N, and ^{16}O ion beams forming a spread-out Bragg peak", Med. Phys. **38**, 6585-6591 (2011).

[31] GATE Collaboration, www.openGATEcollaboration.org/.

[32] GEANT4, http://GEANT4.cern.ch/.

[33] L. Grevillot, T. Frisson, N. Zahra *et al.*, "Optimization of GEANT4 settings for proton pencil beam scanning simulations using GATE" Nucl. Instr. Meth. Phys. Res. **268**, 3295-3305 (2010).

[34] E. Haettner, H. Iwase, M. Krämer, G. Kraft and D. Schardt, "Experimental study of nuclear fragmentation of 200 and 400 MeV/u ^{12}C ions in water for applications in particle therapy", Phys Med Biol. **58**, 8265-8279 (2013).

[35] D. Schardt, T. Elsässer and D. Schulz-Ertner, "Heavy-ion tumor therapy: Physical and ra-

diobiological benefits", Rev. Mod. Phys. **82**, 383-425 (2010).

[36] D. Jette and W. Chen, "Creating a spread-out Bragg peak in proton beams", Phys. Med. Biol. **56**, 131-138 (2011).

[37] J. J. Wilkens and U. Oelfke, "Direct comparison of biologically optimized spread-out bragg peaks for protons and carbon ions", Int. J. Rad. Oncol. Biol. Phys. **70**, 262-266 (2007).

[38] Y. Prezado, I. Martínez-Rovira, S. Thengumpallil and P. Deman, "Dosimetry protocol for the preclinical trials in white-beam minibeam radiation therapy", Med. Phys. **38**, 5012-5020 (2011).

[39] H. Zhang, H. Zhong, R. F. Barth, M. Cao and I. J. Das, "Impact of dose size in single fraction spatially fractionated (grid) radiotherapy for melanoma", Med. Phys. **41**, 021727 (2014).

[40] E. Mori, A. Takahashi, N. Yamakawa, T. Kirita, T. Ohnishi, "High LET heavy ion radiation induces p53-independent apoptosis", J Radiat Res. **50**, 37-42 (2009).

[41] P. Mehnati, S. Morimoto, F. Yatagai, Y. Furusawa, Y. Kobayashi, S. Wada, T. Kanai, F. Hanaoka and H. Sasaki, "Exploration of "over kill effect" of high-LET Ar- and Fe-ions by evaluating the fraction of non-hit cell and interphase death", J Radiat. Res. **46**, 343-350 (2005).

[42] W. K. Weyrather, S. Ritter, M. Scholz and G. Kraft, "RBE for carbon track-segment irradiation in cell lines of differing repair capacity", Int J Radiat Biol. **75**, 1357-1364 (1999).